J. Fluid Mech. (1994), *vol.* 280, *pp.* 173–197

Joint statistics of a passive scalar and its dissipation in turbulent flows

By F. ANSELMET, H. DJERIDI AND L. FULACHIER

Institut de Mécanique Statistique de la Turbulence, Unité Mixte N° 380033 Université d'Aix-Marseille II/CNRS, 12, avenue Général Leclerc, 13003 Marseille, France

(Received 8 July 1993 and in revised form 20 June 1994)

The statistical relationship between a passive scalar and its dissipation is important for both a basic understanding of turbulence small-scale properties and for various aspects of turbulent combustion modelling. This problem is studied in two different flows through spectral analysis as well as probability density functions using temperature as a passive scalar. Particular attention is paid to the experimental determination of the three squared derivatives involved in the temperature dissipation. As a first step, it is found that basic properties such as the correlation coefficient between temperature and its dissipation are strongly related to the asymmetry of the scalar fluctuations, so that the usually assumed statistical independence between these variables is not justified. These trends are the same for the two flows investigated here, a boundary layer and a jet. This connection appears to be related to fluctuations of small amplitude for both quantities which are associated with relatively low frequencies lying between the integral scale and the Taylor microscale. In regions where the temperature skewness factor is nearly zero, the correlation coefficient is also very small, and several tests show that the assumption of independence is then fully justified. Thus, the main parameter influencing joint statistics of temperature and its dissipation is the asymmetric feature of temperature fluctuations, but the asymmetry of the longitudinal temperature derivative, which results from the flow boundary conditions and is usually felt through the presence of the so-called temperature ramps, is also involved. Even though the magnitude of the derivative skewness factor is almost uniformly distributed in both flows, the secondary effect becomes the dominant one in flow regions where the influence of the temperature asymmetry is relatively weak.

1. Introduction

Over the last decade, much attention has been paid both experimentally and numerically to the turbulent transport of scalars, partly because of the relevance of these studies to the problems related to turbulent combustion and partly because quite unexpected properties have appeared. For instance, it was shown that, even though passive scalars do not affect the velocity field structure, such scalars cannot so far be completely determined from our present knowledge of the velocity field turbulence mixing properties. For instance, the study of heated grid-generated turbulence performed by Warhaft & Lumley (1978) has clearly shown that even in this basic situation the passive scalar properties (such as the temperature variance decay rate or the dissipation characteristics) strongly depend on its initial conditions. Indeed, Bilger (1989) has underlined in a quite recent review paper of turbulent combustion problems that new results 'improving our understanding of turbulent transport and mixing of scalars, including the structure of scalar-dissipation fields' are eagerly awaited even

when these scalars are not involved in chemical reactions and when they are passive contaminants.

The mean value $\overline{\epsilon_\theta}$ of the scalar dissipation (e.g. the destruction rate of half the scalar variance $\frac{1}{2}\theta'^2$) is an important quantity which appears in various modelling approaches of turbulent flows. But the crucial role of the scalar dissipation rate also appears in the probability density function (p.d.f.) models which were initially developed for solving combustion problems: it is at present well known that in both premixed (Bray 1980) and diffusion (Bilger 1980) flames, the average rate of creation or destruction of chemical species can be related to the joint probability density function (j.p.d.f.) of an inert contaminant θ and its dissipation ϵ_θ. In a more recent model of turbulent reacting flows based on the variation through the flow field of averages of quantities, such as species mass fractions, conditional on mixture fraction, the conditional square gradient appearing in the diffusion mixing term has also to be modelled (Bilger 1993). Similarly, the flamelet modelling of non-premixed flames recently tested by Vranos (1992) requires an assumption for the j.p.d.f. of the local mixture fraction and its dissipation rate since this quantity is used for linking the separately performed calculations of the laminar flamelets and of the underlying turbulent field. Statistical independence has so far been assumed. On a more general basis, the mapping closure technique (Chen, Chen & Kraichnan 1989), worked out to describe the mixing of scalars in various turbulent fields, also showed that one of the main problems lies in the modelling of the conditional scalar dissipation, which is directly connected to the j.p.d.f. of the scalar and its dissipation. It has been proved (Gao 1991) that, for a Gaussian field, the two quantities are statistically independent, but the well-known problem of achieving relaxation of initially binary statistics to Gaussianity has so far not been resolved (O'Brien & Sahay 1992). In other models associated with the p.d.f. formulation (e.g. Borghi & Gonzalez 1986; Pope & Chen 1990), length or time scales are also related to the j.p.d.f. of an inert scalar and its dissipation.

Most of the studies devoted to dissipation have been concerned with mean-squared derivatives in connection with local isotropy and/or axisymmetry assessment. However, Namazian, Scheffer & Kelly (1988) obtained dissipation statistics in the developing region of an isothermal methane jet issuing into still air using Raman scattering showing that, in the shear layer near the jet exit, the scalar and its dissipation are highly correlated. Such a strong correlation is in opposition to Bilger's (1976) conjecture that θ and ϵ_θ might be statistically independent so that their j.p.d.f. can be replaced by the product of the marginal p.d.f.s. This result also seems different from that obtained by Anselmet & Antonia (1985) in a weakly heated turbulent plane jet: iso-j.p.d.f. contours between temperature and an approximation to ϵ_θ evaluated from the temperature temporal derivative are roughly similar to the contours of the product of the marginal p.d.f.s. Nevertheless, when these results are thoroughly examined (Anselmet & Antonia 1985, figure 5, p. 1052), it is obvious that this hypothesis is strictly verified only where the skewness S_θ of temperature fluctuations is practically zero and the intermittency factor γ is about 1; on the axis, where $S_\theta \approx -0.8$ and $\gamma = 1$, the assumption of independence is much less justified. Thus, one may wonder whether the statistical independence between θ and ϵ_θ is related to the symmetry of temperature fluctuations. A similar trend is observed in direct numerical simulations of the turbulent mixing of a passive scalar (Eswaran & Pope 1988) where it is found that the conditional scalar dissipation $\langle \epsilon_\theta / \theta = \theta_0 \rangle$ (for a given value θ_0 of θ) is strongly dependent on θ_0 for small times corresponding to a bimodal p.d.f. of θ, and becomes independent of θ_0 at long times when the θ-distribution tends to a Gaussian. These results are also related to the recent experimental study by Jayesh & Warhaft (1992)

showing, in grid-generated turbulence with a linear mean temperature gradient, very large conditional scalar dissipation rates associated with the temperature fluctuations corresponding to the observed p.d.f. exponential tails.

In addition to the scalar field asymmetry, a relevant feature may be the intermittent character of some regions of the flow: what is happening when intermittency is strong, i.e. $\gamma \ll 1$? And, more generally speaking, are there any other local or global flow characteristics influencing the link between a passive scalar and its dissipation? In order to analyse a turbulent flow which has regions where the skewness of scalar fluctuations strongly differs from zero with one of them where, in addition, the intermittency factor strongly departs from unity, a weakly heated boundary layer has been first studied. Experimental techniques for measuring the dissipation fluctuations were first thoroughly tested in this flow as the wire lengths, their relative spacing, and other parameters may strongly affect such measurements. Then, a second flow, a slightly heated jet, was studied in order to check the universality of results obtained in the boundary layer as these flows present some very different features. We will mainly discuss results obtained at three typical positions in each of the boundary layer and jet flows for which joint statistics of temperature and its dissipation significantly differ.

For the boundary layer, the expression for ϵ_θ is

$$\epsilon_\theta = D\left[\overline{\left(\frac{\partial\theta}{\partial x}\right)^2} + \overline{\left(\frac{\partial\theta}{\partial y}\right)^2} + \overline{\left(\frac{\partial\theta}{\partial z}\right)^2}\right] = \epsilon_{\theta x} + \epsilon_{\theta y} + \epsilon_{\theta z}, \tag{1}$$

where D is the thermal diffusivity, x the streamwise distance, y the normal to the wall one and z is along the spanwise direction. In order to simultaneously determine these gradients, a four-wire probe is necessary since the longitudinal derivative is inferred from the temporal one using Taylor's hypothesis. The optimal dimensions of that probe were determined from a systematic study using two-wire probes. Section 2 will briefly recall the main characteristics of the two flows and the measurement methods, and §3 will report the results on the joint statistics of temperature and its dissipation obtained from the combined spectral and probabilistic analyses.

2. Experimental arrangement

Only a brief description of the experimental procedures will be reported here since a thorough description of both the flow characteristics and the determination of the probe configurations is reported in Anselmet, Djeridi & Fulachier (1994). The reader may also refer to Djeridi (1992).

2.1. *Experimental facilities*

2.1.1. *Boundary layer flow*

The turbulent boundary layer develops on the working section floor of a low-speed wind tunnel and its characteristic properties have already been studied in detail (e.g. Fulachier 1972; Antonia *et al.* 1988). The wall is heated to a constant temperature Θ_w from the beginning of the layer such that the difference with respect to the ambient temperature Θ_e is 10 K and heat is acting as a passive scalar. At the measurement station, the free-stream velocity is $U_e = 12\ \mathrm{m\ s^{-1}}$, the boundary layer thickness is $\delta = 62$ mm and the momentum thickness Reynolds number is 4900. The friction velocity and temperature are $u^* = 0.46\ \mathrm{m\ s^{-1}}$ and $\theta^* = 0.47$ K respectively. Profiles for the mean and fluctuating velocity and temperature fields are in very good agreement (e.g. Antonia *et al.* 1988) with the standard ones throughout the boundary layer.

Values of the Kolmogorov lengthscale η vary from about 0.1 mm in the wall region to 0.5 mm in the outer part of the flow. The associated frequencies $f_k (= U/2\pi\eta)$ are about 2.5 KHz very close to the wall at the limit position where measurements could be made $y^+ = 3$ ($y^+ = yu^*/\nu$ with ν, kinematic viscosity), 12 KHz at $y^+ \approx 180$, in the region where it is maximum, and 4 KHz in the outer part of the boundary layer. The Reynolds number R_λ defined with respect to the Taylor microscale λ_g and the r.m.s. of the longitudinal velocity fluctuations is almost constant within the boundary layer, with a value of about 130.

2.1.2. *Jet flow*

The jet flow is obtained from a fully developed turbulent pipe flow (primary flow, mean axis velocity $U_j = 12\ \mathrm{m\ s^{-1}}$) discharging into ambient air (secondary flow, $U_e = 1.2\ \mathrm{m\ s^{-1}}$) in a slightly confined configuration. The Reynolds number $R_j = U_j D_j/\nu$ is then about 21 000 (where $D_j = 26$ mm is the nozzle diameter). The exit temperature difference between the primary and secondary flows is $\Theta_j - \Theta_e = 20$ K. The main characteristics of this flow are in good agreement with the usual ones for the axial mean velocity and temperature difference fall-offs, the jet half-width growths and the turbulent velocity field main properties (Amielh *et al.* 1994). However, as they could not be measured in a systematic way, the dissipation field characteristic length and frequency scales were estimated using a second-order model developed in parallel to the experimental work performed in this jet facility (Ruffin *et al.* 1994). The jet exit value ($\eta = 0.005 D_j$) corresponds very closely what is usually found in turbulent pipe or channel flows, $\eta \approx 0.0053 D_j$. This value is constant until $X/D_j \approx 4$, with f_k about 15 $\mathrm{KH_z}$ and R_λ about 100. Then, η goes through a minimum value attained at $X \approx 8D_j$ where $\bar{\epsilon}$ reaches its maximum centreline value and f_k is much greater than 10 KHz: measurements with fine wires are as yet impossible in this region. At the downstream station $X = 15D_j$ where most of the experiments reported are performed, η on the jet axis is about 0.1 mm, with f_k about 9 KHz and R_λ about 200. At the same station, away from the axis, η is almost the same as on the centreline since radial variations of $\bar{\epsilon}$ are very small, at least in regions where intermittency is not large. However, at the off-axis position ($X = 15D_j$ and $R = 2D_j$) where detailed results will also be reported in this paper, the intermittency factor is about 0.3, $\bar{\epsilon}$ is about 10 times smaller than on the centreline and η is then about 0.17 mm. At this station, the velocity half-width is about 30 mm so that $R = 2D_j$ corresponds to a distance slightly larger than twice the jet half-width.

It is interesting to mention that an important difference exists between the boundary conditions for the jet flow and the boundary layer, which appears to play a role in some of the results reported in this paper. Indeed, for the former case, large velocities correspond to large temperature values (on the jet axis) whereas small velocities correspond to small temperature values (in the regions far from the axis). On the other hand, for the latter case, large velocities correspond to small temperatures in the outer region, and vice versa in the wall region. This difference is known to affect the small-scale statistics of the temperature field (e.g. Mestayer *et al.* 1976). In addition, the jet flow is characterized by turbulence intensities significantly larger than those generally encountered in the boundary layer, but the conditions are generally much closer to isotropic ones than those for the boundary layer.

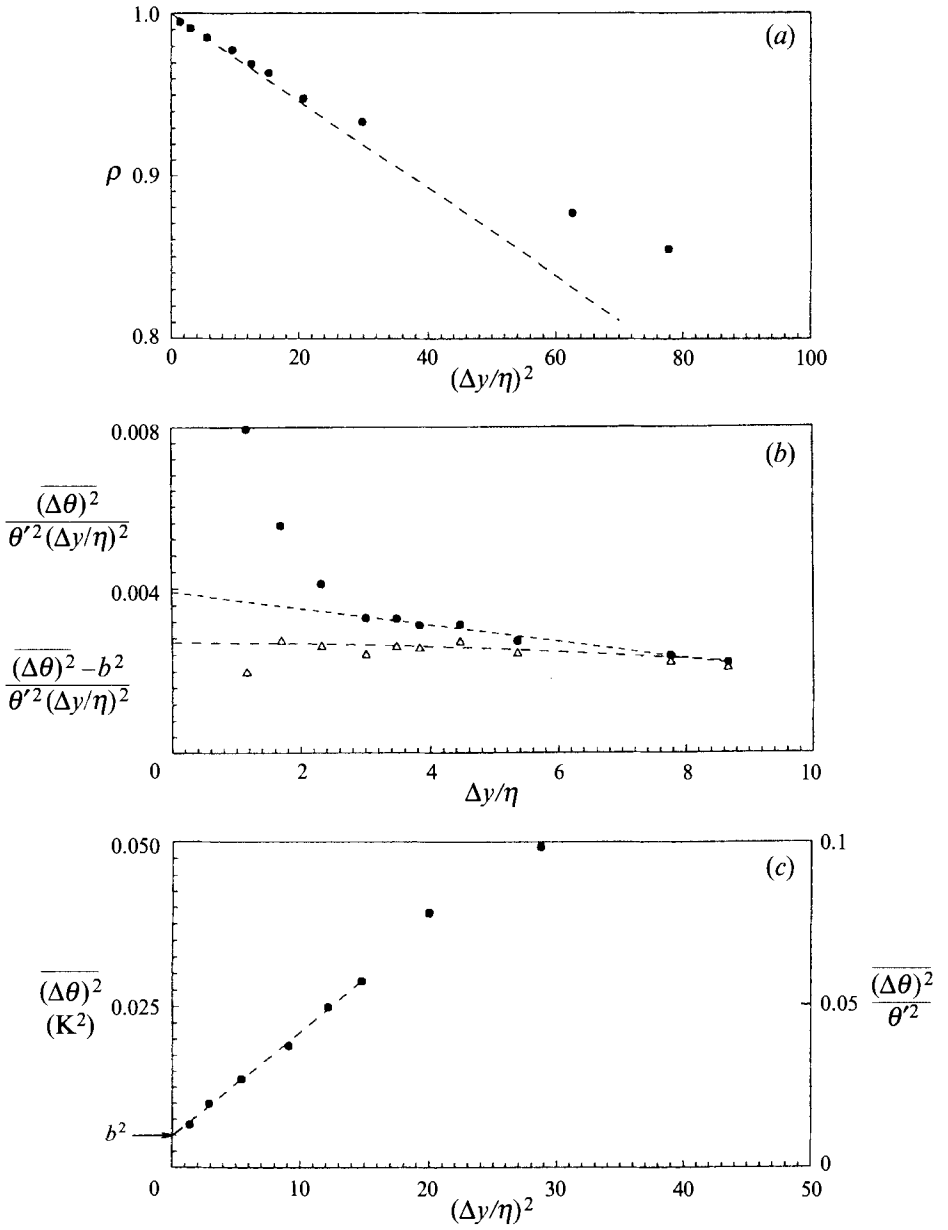

FIGURE 1. Determination of the temperature mean-squared derivative using pairs of wires, obtained in the boundary layer at $y^+ = 180$ for the direction normal to the wall. (*a*) Temperature correlation coefficient for small separations. (*b*) Determination of the ratio $\overline{(\theta(y+\Delta y)-\theta(y))^2}/\Delta y^2$ for different wire spacings; ●, raw data; △, data corrected for 'noise' level. (*c*) Evolution of the temperature difference $\overline{(\theta(y+\Delta y)-\theta(y))^2}$ for the estimation of the 'noise' level.

2.2. *Probe arrangements*

2.2.1. *One-wire probes: determination of the longitudinal derivative*

Temperature fluctuation measurements are performed with cold wires (Pt–10% Rh) of diameter d equal to 0.63 μm operated with in-house constant-current circuits. The heating current is equal to 0.2 mA such that the velocity sensitivity of the wire is

practically negligible and the signal-to-noise ratio is large enough to allow correct dissipation measurements. Since fine wires are used, the wire time constant M is very small. For instance, in the boundary layer, for $y^+ = 3$ corresponding to the measurement point closest to the wall and the most critical situation, M is about 30 μs. The time constant M has been evaluated using the usual relation available in the literature (e.g. Fulachier 1978). This results in a cut-off frequency of 5 KHz to be compared with the Kolmogorov frequency f_k about 2.5 KHz. At $y^+ \approx 180$, in the region where f_k is a maximum, these frequencies are equal to 8 KHz and 12 KHz respectively. For results presented herein no correction is made to take into account the influence of M. Indeed, it appears that the main problem is related to the spatial integration resulting from the wire length ($l \approx 0.35$ mm), which is about 4η close to the wall ($y^+ = 2.4$) and about 3η at $y^+ = 180$. Such wire lengths are consistent with those used by Krishnamoorthy & Antonia (1987), i.e. $l/\eta = 4.5$ at $y^+ = 180$, and those recommended by Wyngaard (1971) whose analysis predicts a 10% attenuation of $\overline{\epsilon_\theta}$ with $l/\eta = 3$. In order to perform fine-scale measurements in the boundary-layer, and especially in the wall vicinity, it is also necessary to compare the wire length to typical lengthscales of this flow: our value ($l^+ \approx 10$) is in good agreement with that recommended by Klewicki & Falco (1990), $l^+ \approx 7$, for measurements of the velocity time derivative skewness, with a momentum Reynolds number equal to the present one.

The longitudinal temperature derivative has been estimated using Taylor's hypothesis which has been validated both experimentally and numerically (e.g. Antonia *et al.* 1984; Piomelli, Balint & Wallace 1989) when turbulence intensities are less than about 20% and is, in addition, the only practical approach for simultaneous measurements of the three temperature derivatives. After testing several methods, the signal time derivative obtained with an analogue circuit was chosen, providing a linear gain variation up to frequencies larger than 50 KHz. Note that a special study has also been performed concerning end-conduction effects which result in a similar attenuation of the temperature and time derivative variances. These problems are discussed in Anselmet *et al.* (1994).

2.2.2. *Multi-wire probes for measurements of the two other derivatives*

In order to determine the two other derivatives, pairs of parallel wires have to be used, and a systematic study is necessary to determine the optimal separation between these wires since spatial resolution problems are quite important for such measurements (e.g. Mestayer & Chambaud 1979). All of these probes are home-made. The prongs are made from piano wires which are tapered to a tip diameter of about 0.2 mm.

The mean values of the squared derivatives are first inferred from the behaviour of the spatial correlation function for small separations (e.g. Verollet 1972; Krishnamoorthy & Antonia 1987). Indeed, a Taylor series expansion of the temperature along any of the directions ξ gives the following expression for the correlation coefficient ρ between temperature fluctuations at two points separated by a distance $\Delta\xi$:

$$\rho(\Delta\xi) = 1 - \tfrac{1}{2}(\Delta\xi)^2\left[\frac{\overline{(\partial\theta/\partial\xi)^2}}{\theta'^2} - \left(\left(\frac{1}{2\theta'^2}\right)^2\right)\left(\frac{\overline{\partial\theta^2}}{\partial\xi}\right)^2\right] + O((\Delta\xi)^3). \tag{2}$$

In the jet flow, the term $((1/2\theta'^2)^2)(\overline{\partial\theta^2}/\partial\xi)^2$ is always negligible, whereas, in the boundary layer, this quantity for $\xi \equiv y$ is the dominant one very close to the wall. Thus, except in the latter region, the parabolic behaviour of the correlation coefficient curve for small wire separations $\Delta\xi$ directly yields the mean-squared derivative value. For the

latter situation, the correction is based on the wall vicinity evolution of the temperature root mean square (e.g. Antonia *et al.* 1988): $\theta'^{+} = 0.26y^{+}$ which is valid in the region very close to the wall.

Figure 1(*a*) shows a typical example at $y^{+} = 180$. The experimental data actually closely follows a parabolic evolution for separations Δy as large as about 5η. However, at positions closer to the wall, this trend is only valid for smaller separations: at $y^{+} = 5$, it only extends to about 3η. This difference may be related to increasing errors in the determination of both the distance between wires and the value of the Kolmogorov lengthscale as these quantities become smaller when getting closer to the wall.

From this set of data ($\theta(\xi, t)$ and $\theta(\xi+\Delta\xi, t)$), one can also infer the difference signals $\theta(\xi+\Delta\xi, t)-\theta(\xi, t)$ and compute their variances. This procedure should be strictly equivalent to that previously discussed. However, figure 1(*b*) clearly shows that additional experimental errors appear when computing the difference signals and this effect gets larger with smaller separations $\Delta\xi$ as the two initial temperature signals become almost identical and calibration and gain errors become more important. Indeed, when only the mean value of the squared temperature difference $\overline{\Delta\theta^2}$ is plotted as a function of the squared separation $\Delta\xi^2$ (figure 1*c*), one notices that the almost linear evolution does not cross to zero when $\Delta\xi^2$ goes to zero. Thus, in a way similar to that proposed by Hannart, Gagne & Hopfinger (1985), one can simply represent this effect through the influence of an additional 'noise' level b^2 which contaminates the data and remains practically constant with varying separation $\Delta\xi^2$. Correcting the $\overline{\Delta\theta^2}$ data from this quantity b^2 yields the second distribution presented on figure 1(*b*), showing that the evolution of $\overline{\Delta\theta^2}-b^2$ with respect to $\Delta\xi^2$ is almost flat and converging to the value inferred from the correlation coefficient procedure (see Anselmet *et al.* 1994 for details).

The optimal separation of pairs of wires, for each position in either of the flows investigated here, is then defined as that for which the measured mean-squared difference has the same value as the dissipation contribution obtained from the correlation coefficient method (see figure 1*b*). These separations lie in the range 3η to 6η in both the boundary layer and the jet. This corresponds from 0.3 to about 2 mm, with the smaller values obtained in the region close to the wall and the larger ones in the outer region of the boundary layer. In the jet, η variations are smaller and the range of separations is narrower. Obviously, these values are likely to depend on both the flow characteristics (including R_λ) and the instrumentation noise level, though we are not aware of a systematic study of this problem. However, we will mention that temperature derivative measurements in a 'pure' jet (i.e. with laminar exit conditions, no co-flow and $R_\lambda = 150$) performed by Antonia & Mi (1993) display trends which are very similar to ours for the optimum wire spacing.

Since it was decided to use a four-wire probe with a fixed geometry in order to reduce the probe blocking effects and make measurements less tedious, the statistical properties of the squared derivative signals as well as their correlation coefficients with temperature obtained with non-optimal spacing have also been analysed but these results are not reported herein (see Anselmet *et al.* 1994 for details). The spacing between the two wires ($l \approx 0.4$ mm) in each pair of parallel wires is about 0.3 mm. In order to account for the non-optimal separations of the wires and to maintain as closely as possible the exact balance between the three contributions to the mean total dissipation, multiplicative factors are applied to the three recorded instantaneous signals. Thus, $\overline{\epsilon_\theta}$ obtained with the four-wire probe is actually equal to the value determined from the two-wire probe measurements.

The various signals are low-pass filtered at the frequency cut-off $f_c = 10$ KHz before

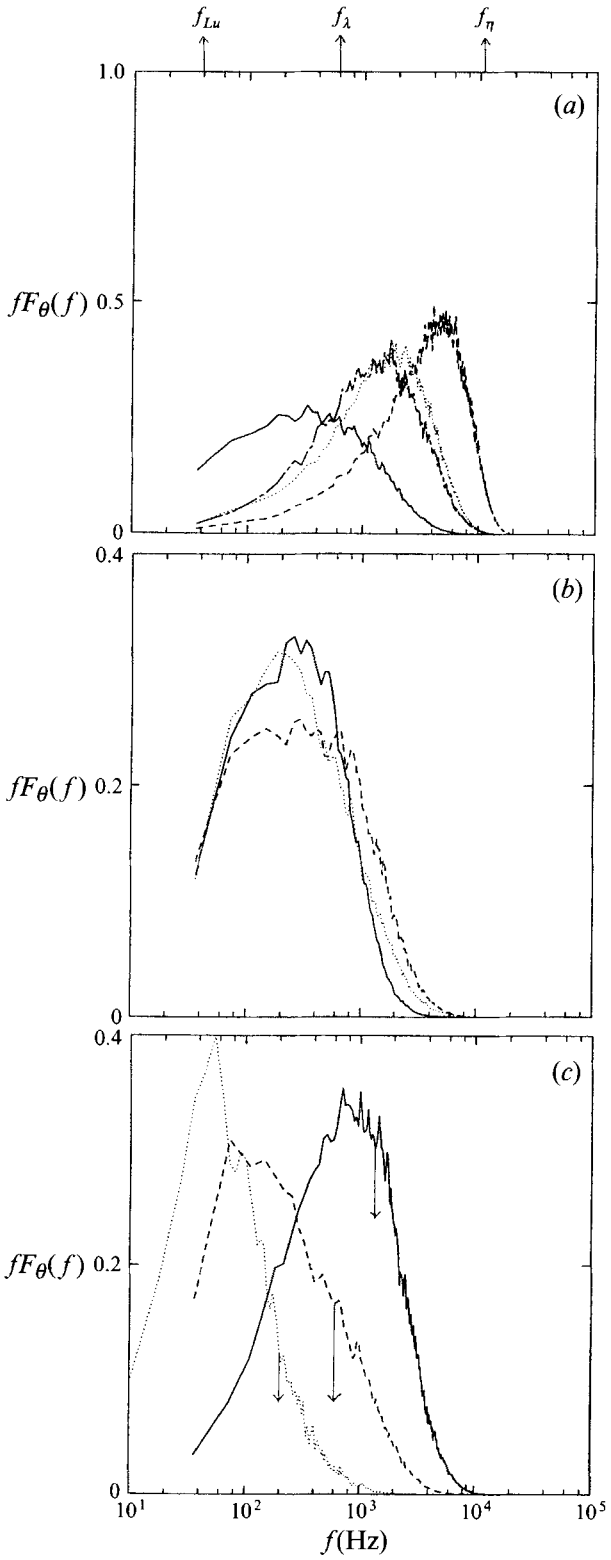

FIGURE 2. For caption see facing page.

on-line digitizing (37.5 KHz/channel). The high-resolution (15 bits with sample and hold systems) A/D converter is connected to a microcomputer where data (1 M-points corresponding to about 14 s duration) are stored.

3. Connection between temperature and its dissipation

As the main objective of this work is to obtain detailed joint statistics of temperature and its dissipation, averaged values of these quantities will not be reported as they are in general good agreement with the classical ones (e.g. Krishnamoorthy & Antonia 1987 for the boundary layer, Antonia, Prabhu & Stephenson 1975 and Panchapakesan & Lumley 1993 for the jet). However, it is necessary to first present spectra and marginal p.d.f.s of the variables studied herein in order to recall the main statistical characteristics of these fields. It is also necessary to mention that, since results reported in this paper show that the connection between temperature and its dissipation is associated with relatively low frequencies – typically lying in the range between the frequencies corresponding to the integral scale and the Taylor microscale – spectral distributions will be plotted on semi-logarithmic scales: such a representation emphasizes the frequencies which are actually contributing most to the variances of the various quantities. In addition, in order to allow easier comparison between results obtained in different flow regions, the scales used for one type of plot will always be the same though calculations may be performed on distinct ranges of variations. This is the case for spectra obtained in the outer region of the jet which are significantly shifted to lower frequencies with respect to the spectral distributions obtained at the other positions. Similarly, j.p.d.f.s obtained in regions where temperature fluctuations are asymmetric are evaluated on significantly different ranges of centred and normalized fluctuations $\alpha = \theta/(\overline{\theta^2})^{1/2} = \theta/\theta'$ (i.e. $[-3;9]$ when $S_\theta > 0$ and $[-9;3]$ when $S_\theta < 0$) though they are presented over the range $[-6;6]$ which is suitable for symmetric conditions. Finally, it is worth mentioning that good statistical convergence was ensured for all results reported hereafter for both the number of analysed samples and the mesh refinement for the evaluation of the j.p.d.f.s, the conditional probabilities and the conditional averages (see Anselmet *et al.* 1994 for details).

3.1. *Flow characteristic features*

Figures 2 and 3 give examples of spectral distributions and probability density functions obtained in the boundary layer and the jet at the typical positions we will mainly pay attention to in the paper. Figure 2(*a*) presents spectra of temperature and its three squared derivatives as determined in the boundary layer at $y^+ = 60$. For information, frequencies associated with the velocity field characteristic lengthscales at this position (integral scale L_u, λ_g and η) are indicated by arrows. Figures 2(*b*) and 2(*c*) present the temperature spectra in the three typical regions of the boundary layer and the jet respectively. It is interesting to note that, in the boundary layer, these three typical spectral distributions are not very different so that f_λ is almost constant (400–600 Hz). On the other hand, in the jet (figure 2*c*), the characteristic frequencies are significantly different for the three typical positions.

FIGURE 2. Typical spectra in the boundary layer and the jet. (*a*) Boundary layer, $y^+ = 60$: ——, θ; – – –, $(\partial\theta/\partial x)^2$; ·····, $(\partial\theta/\partial y)^2$; — · —, $(\partial\theta/\partial z)^2$. (*b*) Boundary layer, θ: ——, $y^+ = 3$; – – –, $y^+ = 60$; ·····, $y^+ = 1450$ (also $y/\delta \approx 0.75$); with $f_{\lambda_g} \approx 400$–$600$ Hz for all three positions. (*c*) Jet, θ: ——, $X/D_j = 3$ (axis); – – –, $X/D_j = 15$ (axis); ·····, $X/D_j = 15$ (off-axis) ($R = 2D_j$); arrows point towards f_λ values. Note that for the off-axis position, FFT's are computed with 8192 points instead of 1024 points.

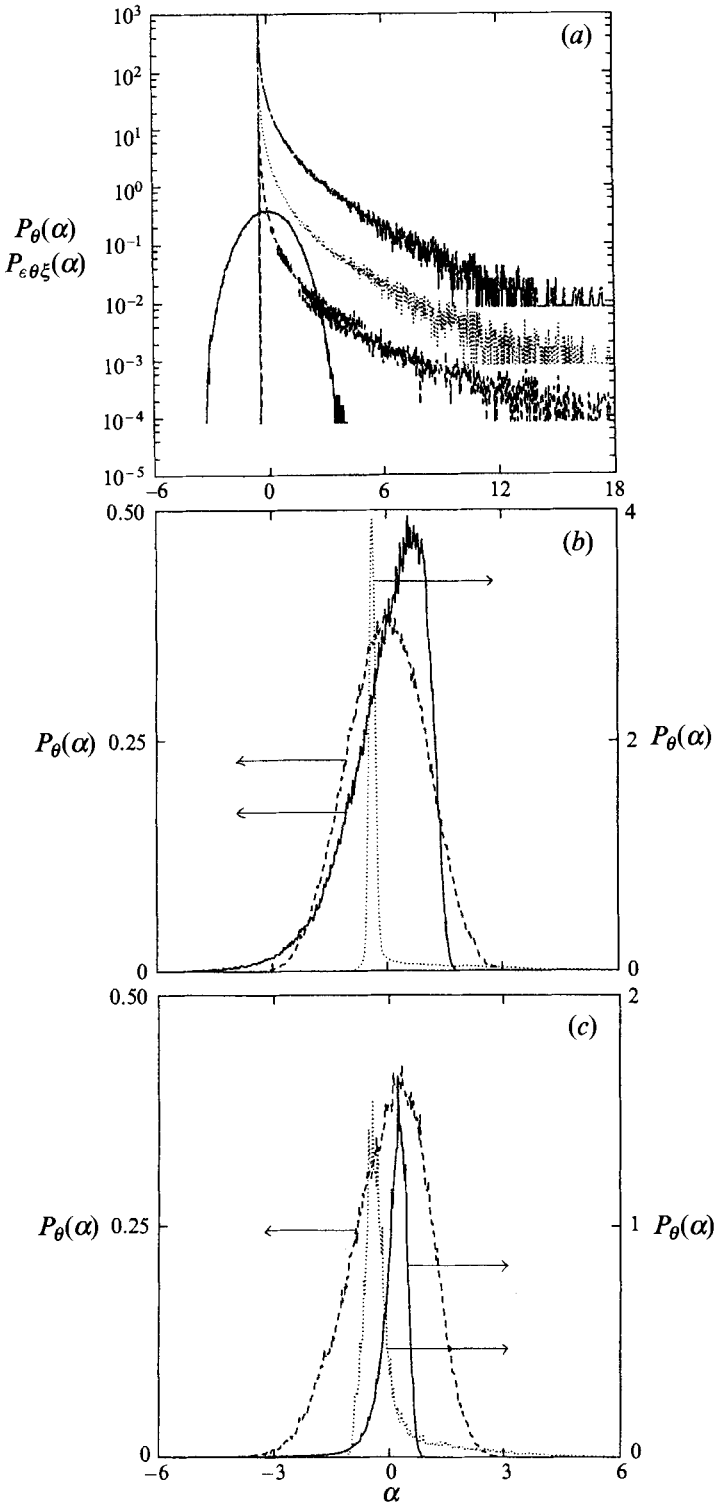

FIGURE 3. Typical probability density functions in the boundary layer and the jet. (*a*) Boundary layer, $y^+ = 60$; ——, θ; – – –, $(\partial\theta/\partial x)^2$; ·····, $(\partial\theta/\partial y)^2$; — · —, $(\partial\theta/\partial z)^2$. The plots for $(\partial\theta/\partial y)^2$ and $(\partial\theta/\partial z)^2$ are shifted upwards one and two decades respectively with respect to the others. (*b*) Boundary layer, θ:——, $y^+ = 3$; – – –, $y^+ = 60$; ·····, $y/\delta \approx 0.75$. (*c*) Jet, θ: ——, $X/D_j = 3$ (axis); – – –, $X/D_j = 15$ (axis); ·····, $X/D_j = 15$ (off-axis).

Figure 3 presents the associated probability distributions plotted as functions of centred normalized fluctuations α. The temperature p.d.f. is symmetrical (skewness = 0) and almost Gaussian (flatness = 2.8) in the inner region of the boundary layer (figure 3*a*, $y^+ = 60$, semi-logarithmic scales) and the well-known intermittent nature of squared derivatives is obvious, with very frequent small fluctuations with respect to the mean value and rare strong positive fluctuations. On the other hand (figure 3*b*), the temperature p.d.f.s are asymmetric in the wall vicinity and, especially, the outer region of the boundary layer. This is particularly important in the outer region where the peak value of the temperature p.d.f. is almost equal to 4 at $y/\delta \approx 0.75$. Consequently, the temperature skewness factor S_θ significantly differs from zero close to the wall and in the outer region, with negative values for the former case and positive ones for the latter case. Similar behaviour is obtained in the jet (figure 3*c*), with an almost symmetrical temperature p.d.f. on the centreline at $X = 15D_j$ and asymmetrical ones at the two other positions. However, the distribution in the outer region at $X = 15D_j$ is much less peaky than that previously presented in the boundary layer, in spite of a smaller intermittency factor ($\gamma \approx 0.3$). This is probably mainly due to the molecular diffusion smoothing effect as, for the jet flow, the secondary non-heated flow is in direct contact with the heated primary flow as early as the very first station where the pipe flow is discharging into the ambient air. On the other hand, in the boundary layer, the heated fluid originating from the wall region is never in direct contact with that of the outer flow, and the molecular diffusion effect is then much smaller. Indeed, since the contributions to the positive skewness factor are associated with positive temperature fluctuations of large amplitude ($\alpha \geqslant 2$), this 'smoothing effect' on the peak of the p.d.f. is practically negligible and the skewness factor is actually slightly larger in the outer region of the jet ($S_\theta \approx 3.5$ for $R = 2D_j$) than in the outer region of the boundary layer ($S_\theta \approx 1.2$ at $y^+ = 1450$, or $y/\delta \approx 0.75$).

3.2. *Global statistics*

In order to study the link between temperature and its total dissipation or any of its contributions (or components), their correlation coefficients ρ were first determined. Figures 4(*a*) and 4(*b*) present these evolutions as determined in the boundary layer and the jet respectively, together with the temperature skewness S_θ and the intermittency factor γ. The main global feature in both flows is that, regardless of the quantity considered for dissipation, the correlation coefficient has the same sign as the skewness factor and, when S_θ significantly differs from zero, ρ also does. For instance, in the boundary layer, close to the wall, ρ and S_θ are both rather strongly negative, whereas they reach quite large positive values in the outer part of the boundary layer ($S_\theta = 3$ for $y^+ = 1700$, or $y/\delta \approx 0.9$, where the intermittency factor γ is about 0.3). On the other hand, in the inner region, ρ and S_θ are both almost equal to zero. However, figure 4(*b*) shows that the zero-crossing points for these two quantities are not exactly the same since, for instance, in the jet at $X/D_j = 15$, S_θ is zero at $2R/D_j \approx 1.8$ whereas $\rho_{\theta,\epsilon\theta x}$ is zero at $2R/D_j \approx 1$. At $X/D_j = 15$, on the jet axis, S_θ is about -0.4 and $\rho_{\theta,\epsilon\theta x}$ is about -0.05, whereas, at the off-axis position ($2R/D_j = 4$), these values are 3.5 and 0.2. Also note that, at this latter position, $\rho_{\theta,\epsilon\theta}$ is as large as 0.4. These results showing that ρ is almost independent of the quantity considered to represent dissipation, and especially in the boundary layer, are quite unexpected since, for instance, isotropic relations for the mean-squared derivatives are far from satisfied in the near-wall region of the boundary layer. In addition, it is now well known that spectral content (e.g. figure 2*a*)

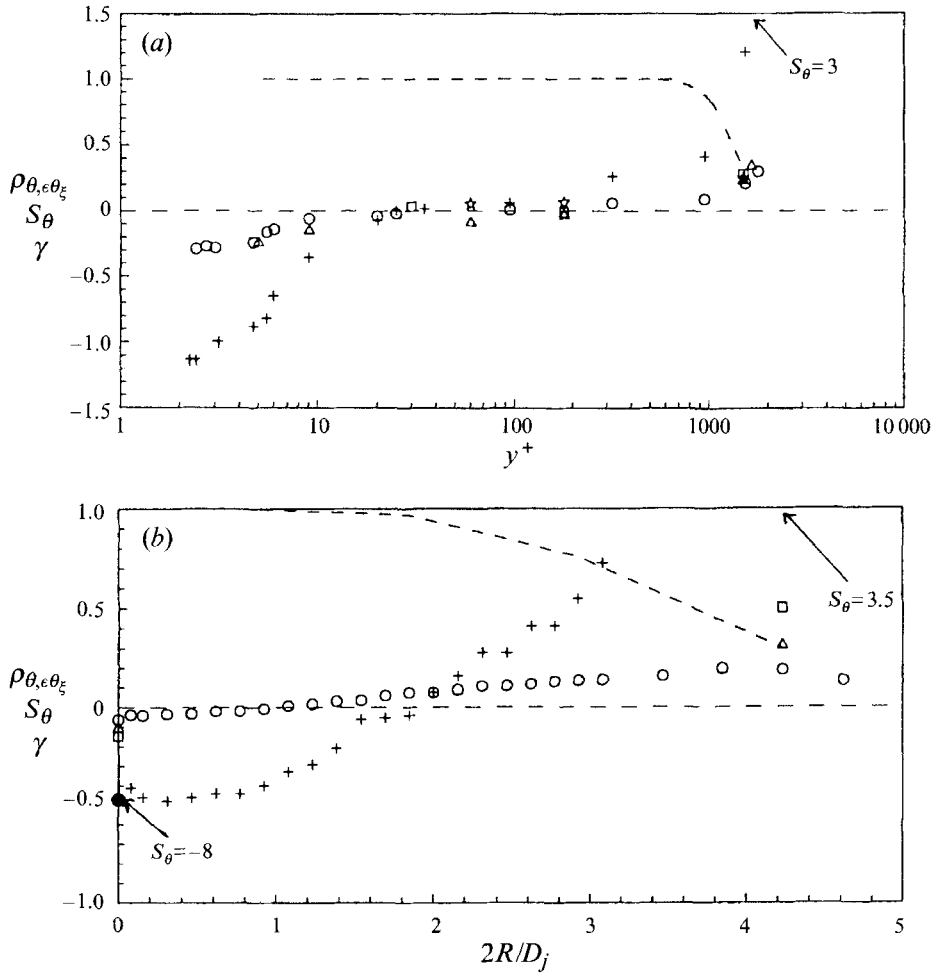

FIGURE 4. Distributions of correlation coefficients between temperature and its dissipation. (*a*) Boundary layer. (*b*) Jet. ○, $\rho_{\theta,\epsilon\theta x}$; △, $\rho_{\theta,\epsilon\theta y}$ or $\rho_{\theta,\epsilon\theta r}$; ☆, $\rho_{\theta,\epsilon\theta z}$ or $\rho_{\theta,\epsilon\theta\phi}$; □, $\rho_{\theta,\epsilon\theta}$; +, S_θ; ——, γ for distributions in the boundary layer and at $X/D_j = 15$; ●, $\rho_{\theta,\epsilon\theta x}$ for $X/D_j = 3$ (axis).

or probability density functions (e.g. Sreenivasan, Antonia & Danh 1977) of the squared gradients can significantly differ from one another.

3.3. *Frequency contributions*

In order to investigate the contribution of individual frequencies f to ρ, cospectra Co (such that $\int Co\,df = \rho$) between θ and any of its dissipation components were computed. Distributions corresponding to ϵ_θ (or $\epsilon_{\theta x}$ in the wall vicinity and at $X/D_j = 3$ in the jet) are shown for typical positions in the boundary layer (figure 5*a*) and the jet (figure 5 *b*). From now on, one distribution only will be given for each typical region since similar results are obtained for the other contributions to ϵ_θ as can be expected from correlation coefficients previously presented. For $y^+ = 3$ and $y/\delta \approx 0.75$, the contributions to ρ are due to rather low frequencies of about the same magnitude as the frequencies providing the most energetic contribution to the temperature variance: this frequency range lies between the value corresponding to the macroscale and that related to the Taylor microscale. It is also interesting to note that, for larger frequencies

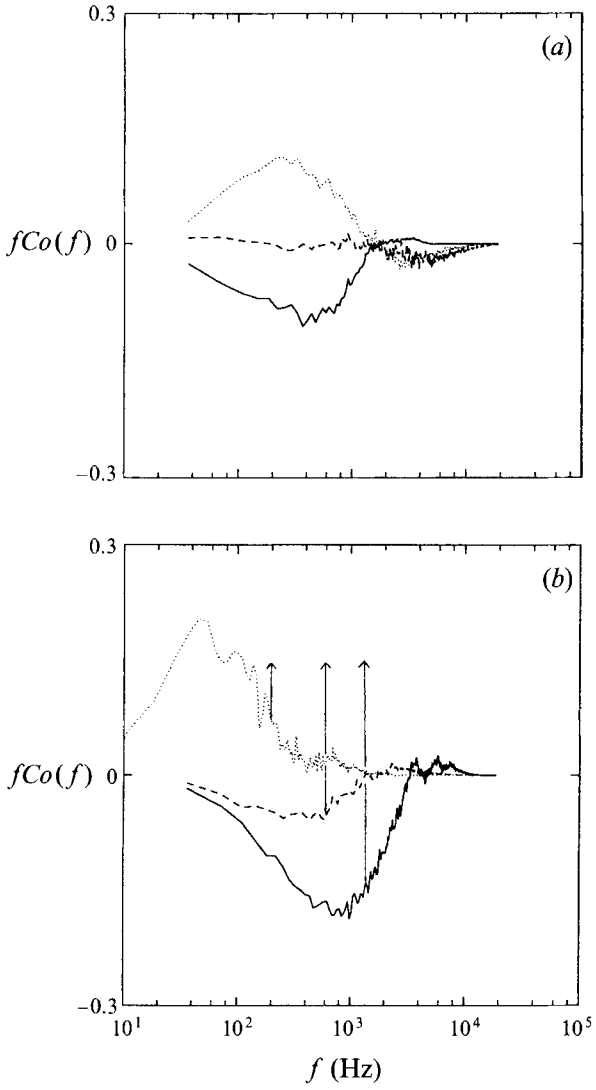

FIGURE 5. Cospectra between temperature and its dissipation. (*a*) Boundary layer: ——, $y^+ = 3$; – – –, $y^+ = 60$; ·····, $y/\delta \approx 0.75$; with $f_\lambda \approx 400$–600 Hz for all three positions. (*b*) Jet: ——, $X/D_j = 3$ (axis); – – –, $X/D_j = 15$ (axis); ·····, $X/D_j = 15$ (off-axis); arrows point towards f_λ values.

(i.e. $f > 1$ KHz), cospectra have a small magnitude but they systematically tend to change sign. Similar behaviour is obtained in the jet at positions (on the axis at $X/D_j = 3$ and off-axis at $X/D_j = 15$) where the correlation coefficients significantly differ from zero, but the frequency range differences already observed for the temperature spectra (figure 2*c*) are then also clearly visible. These trends are practically independent of the direction of the derivative (not shown here, see Djeridi 1992). At positions where ρ is close to zero ($y^+ = 60$ and on the axis at $X/D_j = 15$), the cospectrum is small whatever the frequency. When these cospectra are normalized, for each frequency, by the associated spectra in order to obtain filtered correlation coefficients Cf, the trends are globally quite similar to those reported on figure 5 and these filtered correlation coefficients can be very strong, as large as 0.8 for small frequencies lying between f_{Lu} and f_λ.

3.4. *Joint probability analysis*

Another way to investigate the interdependence between θ and ϵ_θ is to analyse their j.p.d.f. Figure 6 shows iso-contours of the j.p.d.f. $P_{\theta,\epsilon\theta}(\alpha,\beta)$ (where α and β represent the centred and normalized fluctuations of θ and ϵ_θ respectively) for the same typical positions as before in the boundary layer only, as results for the jet are quite similar according to the correlation coefficient values reported on figure 4. In order to give more insight into the rare but very strong dissipation fluctuations which are known to be crucial for other small-scale properties (e.g. Gagne 1987), the contours represented here correspond to levels following a logarithmic increment. Note that these j.p.d.f.s were evaluated with a mesh grid of 100×100 boxes covering the ranges $[-6;6]\times[-2;28]$ r.m.s. at $y^+=60$, $[-9;3]\times[-2;28]$ r.m.s. at $y^+=3$ and $[-3;9]\times[-2;28]$ r.m.s. at $y/\delta\approx0.75$ but results are all presented on the same range ($[-6;6]\times[-2;18]$ r.m.s.) to allow easier comparison between them. These plots are quite similar to those already reported in a heated plane jet for an approximation to ϵ_θ by Anselmet & Antonia (1985). However, these distributions show that the various magnitudes of dissipation fluctuations are clearly influenced by temperature fluctuations α when these are not symmetrically distributed. Indeed, dissipation is almost symmetrically distributed with respect to α when the temperature skewness S_θ is close to zero ($y^+=60$, figure 6*b*) for both small and large levels of the j.p.d.f. On the other hand, when S_θ significantly differs from zero, high-probability contours (associated with small dissipation fluctuations β) are considerably skewed away from temperature fluctuations corresponding to the underlying boundary condition (i.e. 'cold side', $\alpha<0$, $S_\theta>0$, for $y/\delta\approx0.75$, figure 6*c*, and 'warm side', $\alpha>0$, $S_\theta<0$, for $y^+=3$, figure 6*a*) whereas low-probability contours (associated with large dissipation fluctuations β) are more regularly distributed. However, these latter contours are not symmetrical with respect to the temperature mean value ($\alpha=0$) but they are with respect to quite large positive (for $S_\theta>0$) or negative (for $S_\theta<0$) temperature fluctuations. Nevertheless, it is also worth mentioning that, in any case, the temperature fluctuations of largest magnitude are always associated with very small centred dissipation fluctuations ($\beta\approx0$).

In order to get some insight into the statistical independence of temperature and its dissipation, the corresponding iso-contours for the product of the marginal p.d.f.s for temperature $P_\theta(\alpha)$ and dissipation $P_{\epsilon\theta}(\beta)$ are reported on figure 7. At $y^+=60$, where $\rho\approx0$, the j.p.d.f. iso-contours are practically identical with those of the product of the two marginal p.d.f.s (figures 6*b* and 7*b*), whereas, at $y^+=3$, where ρ is strongly negative, these contours are significantly different (figures 6*a* and 7*a*), especially those corresponding to large dissipation fluctuations. Indeed, for this example ($y^+=3$), assuming statistical independence would result in associating large dissipation with small positive temperature fluctuations corresponding to almost unmixed hot fluid whereas, as previously discussed, at this position, they are mainly associated with quite large negative temperature fluctuations corresponding to already mixed fluid which seems to be physically much more realistic. For the other example ($y^+=60$), both the j.p.d.f. and the product of the marginal p.d.f.s associate large dissipation with temperature fluctuations of small amplitude which is quite natural since this corresponds to well mixed fluid. Similar trends are obtained for the outer region of the boundary layer (figures 6*c* and 7*c*), but the boundary condition then influences the 'cold' side of the temperature p.d.f. Similarly, for the jet, the assumption of statistical independence is actually quite well justified on the centreline at the station $X=15D_j$ where the correlation coefficient $\rho_{\theta,\epsilon\theta}$ is close to zero, but it is far from justified at the

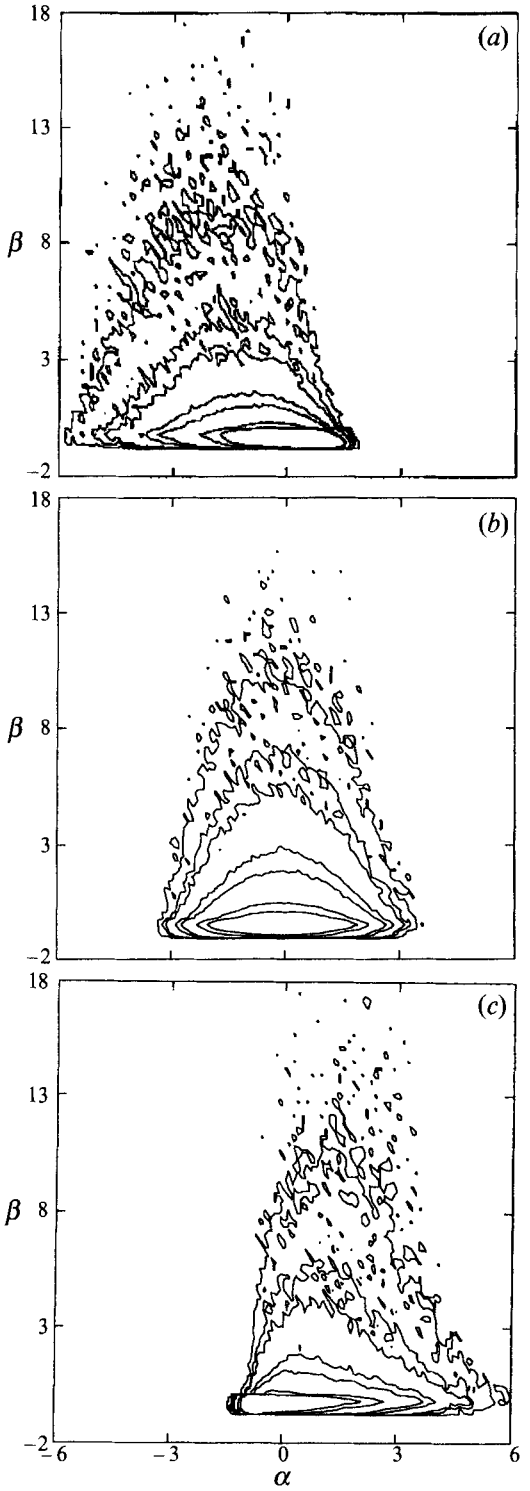

FIGURE 6. Iso-contours for the j.p.d.f. $P_{\theta,\varepsilon\theta}(\alpha,\beta)$ between temperature and its dissipation in the boundary layer. (*a*) $y^+ = 3$; (*b*) $y^+ = 60$; (*c*) $y/\delta \approx 0.75$; outer to inner contours correspond to 0.0001, 0.0005, 0.001, 0.005, 0.01, 0.05 and 0.1.

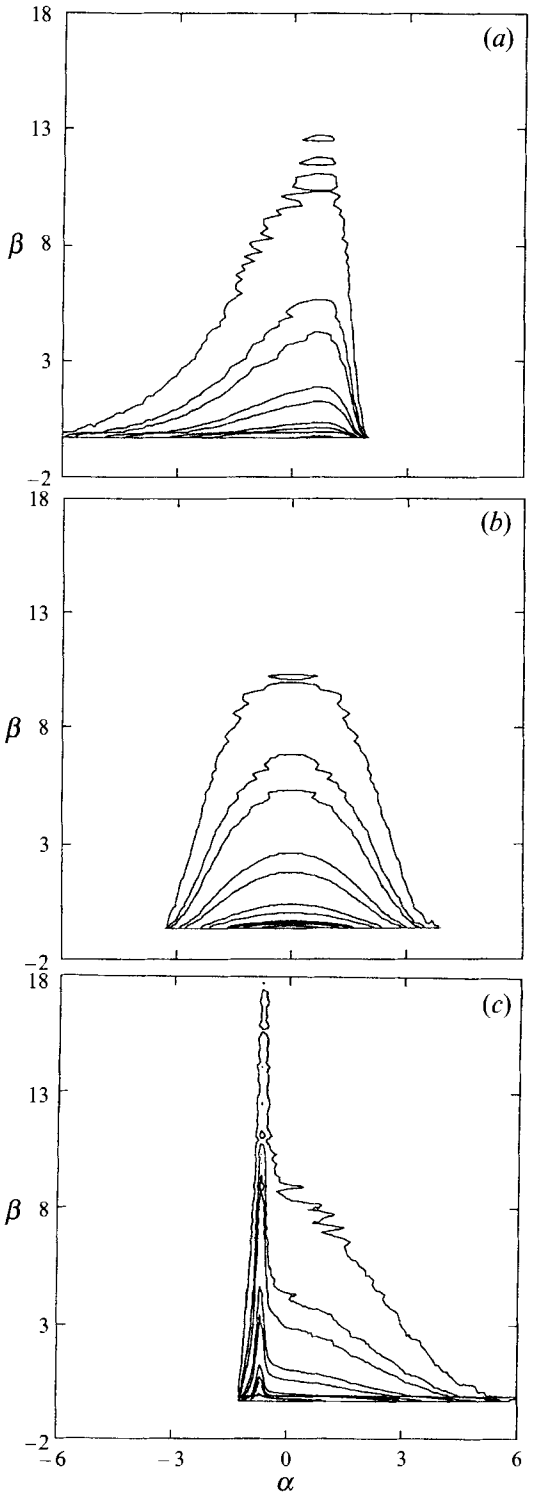

FIGURE 7. Iso-contours for the product $P_\theta(\alpha)P_{\epsilon\theta}(\beta)$ of the marginal temperature and dissipation p.d.f.s in the boundary layer. (*a*) $y^+ = 3$; (*b*) $y^+ = 60$; (*c*) $y/\delta \approx 0.75$; outer to inner contours correspond to 0.0001, 0.0005, 0.001, 0.005, 0.01, 0.05, 0.1, 0.5 and 1.

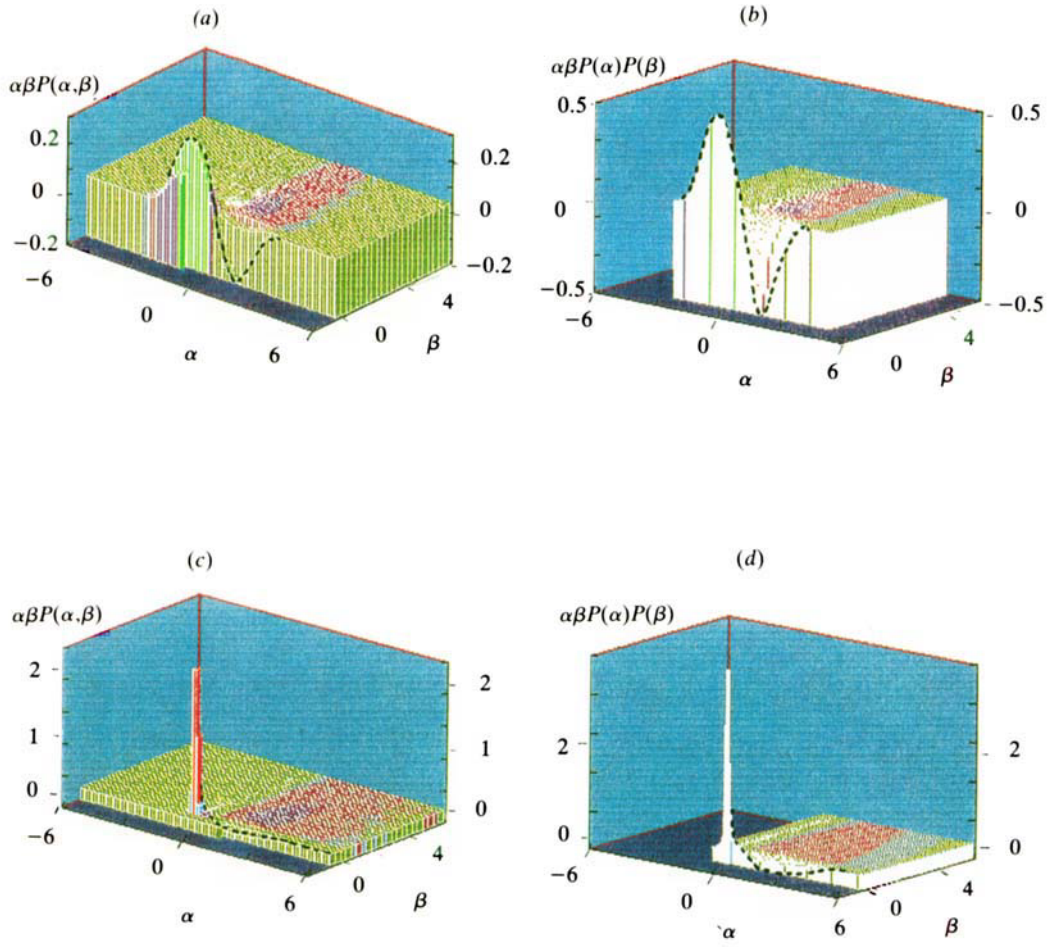

FIGURE 8. Three-dimensional plot of iso-contours for the integrands of the correlation coefficient between temperature and dissipation in the boundary layer. (*a*) $y^+ = 60$, j.p.d.f. $P_{\theta,\epsilon\theta}(\alpha, \beta)$; (*b*) $y^+ = 60$, product of the marginal p.d.f.s $P_\theta(\alpha)P_{\epsilon\theta}(\beta)$; (*c*) $y/\delta = 0.75$; j.p.d.f. $P_{\theta,\epsilon\theta}(\alpha, \beta)$; (*d*) $y/\delta = 0.75$, product of the marginal p.d.f.s $P_\theta(\alpha)P_{\epsilon\theta}(\beta)$.

positions where $\rho_{\theta,\varepsilon\theta}$ is significantly different from zero. Results for much more quantitative tests of independence will be reported later using conditional temperature probabilities and conditional-average dissipation rates.

In fact, the observed statistical independence in regions where the temperature skewness is about zero results from the balance between positive and negative temperature fluctuations which contributes to an almost zero overall correlation coefficient. Iso-contours (presented here on three-dimensional plots, figure 8, plate 1) of the integrands associated with the correlation coefficient between fluctuations α and β, $\alpha\beta P_{\theta,\varepsilon\theta}(\alpha,\beta)$, such that $\int\int \alpha\beta P_{\theta,\varepsilon\theta}(\alpha,\beta)\,\mathrm{d}\alpha\,\mathrm{d}\beta = \rho$, show that (figure 8*a* for $y^+ = 60$), both for positive ($\alpha > 0$) and negative temperature fluctuations ($\alpha < 0$), these contributions significantly differ from zero and they are associated with dissipation fluctuations of very small magnitude lower than the mean value ($\beta < 0$). As expected, very similar behaviour is observed for the products of the marginal p.d.f.s (figure 8*b*). On the other hand, in regions where temperature fluctuations are strongly asymmetric (such as $y/\delta \approx 0.75$, figures 8*c* and 8*d*), where the assumption of independence does not hold at all, it is found that the connection results from the very small dissipation fluctuations ($\beta < 0$) associated with hot fluid ($\alpha > 0$) which is practically unmixed. Obviously, though they are much stronger, the contributions from cold fluid ($\alpha < 0$) associated with large dissipation fluctuations are, on the average, smaller than those from hot fluid since they happen significantly less often. In these regions, the assumption of statistical independence would tend to significantly alter the probability distributions as it was previously discussed, and this would result in the expected exact balance between positive and negative contributions to the integrands $\alpha\beta P_\theta(\alpha)\,P_{\varepsilon\theta}(\beta)$ (figure 8*d*). These findings from the j.p.d.f. analysis, together with those previously discussed which are obtained from cospectra, suggest that the link between temperature and its dissipation is associated with the low-frequency distribution of dissipation fluctuations which are strongly intermittent. Thus, it is interesting to investigate the influence of large-scale intermittency as one can imagine that this feature may strengthen this link since, in non-turbulent portions of signal, temperature and its dissipation will simultaneously be very small.

3.5. *Influence of large-scale intermittency*

In order to check whether the strongly intermittent nature of the flow far away from the wall (at $y/\delta \approx 0.75$ for instance) plays an important role in the previously reported joint statistics between temperature and its dissipation, the probabilistic analysis has been applied again considering only the turbulent portions of the signals. In order to discriminate between turbulent and non-turbulent signal portions, an algorithm was applied to the temperature signal, following a procedure proposed by Jacquin (1983). In fact, it is now well established (e.g. Kuznetsov, Praskovsky & Sabelnikov 1992) that, even for very high Reynolds number flows, velocity is not a precise enough variable for discriminating between turbulent and non-turbulent fluids as there is no sharp boundary between them. When fluctuations with respect to the level corresponding to the outer flow temperature Θ_e are larger than a prescribed threshold and this feature lasts for a lapse of time exceeding another threshold, the associated portion of signal is assumed to lie in a turbulent fluid pocket. The two threshold levels involved in this method are tuned so that the resulting coefficient of intermittency is equal to the classical value (i.e. $\gamma = 0.6$ for that case) and the selected portions of 'turbulent signal' are then the only ones used for computing new statistics. Note that this procedure has first been evaluated with respect to results obtained from the temperature time-squared derivative signal, but using only the temperature signal was easier to implement when

consistency checks associated with the two other quantities $\epsilon_{\theta y}$ and $\epsilon_{\theta z}$ were performed. The sensitivity of the results to the values of the two parameters was quite low and we finally used for this position a threshold level equal to $0.8\theta'$ and a window size equal to 40 points ($= 1.1$ ms $= 7/f_k$). The correlation coefficient ρ is then 0.21 instead of about 0.26 in the non-conditional case. Obviously, intermittency makes the link more pronounced since, in the non-turbulent portions of signal, negative temperature fluctuations with respect to the local mean value of that quantity, which correspond to the outer temperature, are of course always associated with very small negative dissipation fluctuations (β) corresponding to values of that quantity (ϵ_θ) actually equal to zero. Nevertheless, this is not at all the main cause for that link since the 'turbulent signals' are still strongly asymmetric owing to the large amount of cold and almost unmixed fluid. The j.p.d.f.s corresponding iso-contours are not reported here as they are almost identical to those relative to the initial signals.

3.6. *Conditional dissipation rates*

From the j.p.d.f. analysis, one can also compute the conditional centred scalar dissipation, which is an important quantity because, on the one hand, it is a more quantitative way to check statistical independence, and, on the other hand, it appears in the transport equation for the p.d.f. of scalars and has to be modelled. This quantity is defined by

$$\langle(\epsilon_\theta)/\theta = \theta_0\rangle_1 = \int_{-\infty}^{+\infty} \beta P_{\epsilon\theta}(\beta/\alpha_0)\,\mathrm{d}\beta$$

(we will use the notation $\langle\epsilon_\theta\rangle_1$ hereafter for simplicity) and it has the dimension of an average dissipation rate. However, we also report results in the form

$$\langle(\epsilon_\theta)/\theta = \theta_0\rangle_2 = \int_{-\infty}^{+\infty} \beta P_{\theta,\epsilon\theta}(\alpha_0, \beta)\,\mathrm{d}\beta$$

(or $\langle\epsilon_\theta\rangle_2$) though that quantity does not possess the dimension of an average dissipation rate. Indeed, the difference results from the definition of the conditional p.d.f., $P_{\epsilon\theta}(\beta/\alpha_0) = P_{\theta,\epsilon\theta}(\alpha_0, \beta)/P_\theta(\alpha_0)$, and it lies in the values of the probability density function for the various levels α_0 of temperature fluctuations ($\langle\epsilon_\theta\rangle_2 = P_\theta(\alpha_0)\langle\epsilon_\theta\rangle_1$). Thus, the latter quantity $\langle\epsilon_\theta\rangle_2$ is quite meaningful as it gives an insight into the actual contributions to the total average dissipation rate since the probability of occurrence of each realization associated with each level α_0 of temperature is already taken into account. On the other hand, the former quantity $\langle\epsilon_\theta\rangle_1$ does not allow one to quantify the contribution of events to the total average dissipation since their probability of occurrence is not taken into account. Note that, with the normalization adopted in this paper, this integral is in fact equal to zero since all variables are centred with respect to their mean value, i.e. $\int \langle\epsilon_{\theta x}\rangle_2\,\mathrm{d}\alpha_0 = 0$. Indeed, results presented so far clearly show that the main contributions to the correlation coefficients are from small but most frequent fluctuations and not from very large but very rare ones, and we think that both types of results are worth being reported and compared. For instance, results reported for conditional temperature dissipation in grid-generated turbulence by Jayesh & Warhaft (1992) reveal that the large temperature fluctuations corresponding to the p.d.f. exponential tails are associated with large dissipation fluctuations when there is a uniform mean temperature gradient. This is very important for the basic understanding of the flow properties since strong smearing is occurring with the rare strong temperature fluctuations associated with the exponential tails. However, it is not possible to infer from such results the actual contribution of such rare events to the

overall mean statistics of the flow which we believe are very important for modelling the mixing process: indeed it is the quantity $\langle \epsilon_\theta \rangle_2$ which appears in the transport equation for the scalar p.d.f. (e.g. Bilger 1993; Sahay & O'Brien 1993).

In the boundary layer, in the region where temperature fluctuations are almost symmetrical (figure 9*b*, $y^+ = 60$), the θ-p.d.f. is practically Gaussian ($S_\theta = 0$, $F = 2.8$) and the conditional dissipation $\langle \epsilon_\theta \rangle_1$ is quite symmetrically distributed with respect to negative and positive temperature fluctuations. The deviations from one flat distribution are very small as they attain at most the level of the r.m.s. of this quantity, whereas the greatest fluctuations of ϵ_θ can be larger than 20 times the r.m.s. (figure 3). As a consequence of these previous observations, the weighted contribution $\langle \epsilon_\theta \rangle_2$ to the centred mean is also very flat. On the other hand, close to the wall (figure 9*a*, $y^+ = 3$), where the θ-p.d.f. is asymmetrical – owing to the limit resulting from the wall temperature – $\langle \epsilon_\theta \rangle_1$ strongly depends on θ_0, retaining negative values (i.e. almost equal to the 'real zero value' for the non-centred ϵ_θ variable) for positive temperature fluctuations and much larger positive ones for θ_0 negative. The levels of conditional dissipation for negative temperature fluctuations are then much larger – about ten times larger – than those previously discussed for $y^+ = 60$. The trend reported on this figure is of course the same as that obtained from the j.p.d.f. iso-contours (figure 6) but the conditional analysis obviously provides much more quantitative information. A similarly asymmetric feature is observed in the intermittent region (figure 9*c*, $y/\delta \approx 0.75$), but the trends are opposite with respect to those obtained close to the wall and these asymmetries are more clearly marked. This is in agreement with the θ skewness factor S_θ and the correlation coefficient between θ and ϵ_θ which are both larger at $y/\delta \approx 0.75$ owing to strong intermittency which was shown to enhance the correlation (§3.5).

In the jet, results are qualitatively the same for the three typical positions (at $X = 15D_j$) on the centreline where $S_\theta \approx 0$, in the near-field region where $S_\theta < 0$, and at $X = 15D_j$ away from the axis where $S_\theta > 0$ respectively) but they are not reported herein. Note that the distributions presented herein were not smoothed so that we think that the scatter which can be observed in figures 9(*a*) and 9(*c*) reflects convergence problems associated with the evaluation of the tails as a special program with a resolution of 40 boxes for each r.m.s. fluctuation – equal to the resolution used for the computation of the p.d.f.s – was used because direct evaluation from the j.p.d.f.s was obviously not precise enough considering the previously discussed (§3.4) mesh grid resolution we used for the j.p.d.f.s. Thus, the observed oscillations with respect to the average distribution are indicative of the error bars associated with these distributions for large temperature fluctuations ($|\alpha| > 3$). This behaviour corroborates results obtained by Eswaran & Pope (1988) from direct numerical simulations of the turbulent mixing of a passive scalar showing that, for small times corresponding to a bimodal distribution of the scalar, dissipation is strongly dependent on the scalar level under consideration – with very small dissipation associated with the extremal values of the unmixed scalar – whereas, for larger times, when the scalar p.d.f. tends to be Gaussian, dissipation is nearly independent of the scalar level.

3.7. *Additional spectral information*

Other flow properties were also found to affect joint statistics of temperature and its dissipation, but their influence is rather smaller. Indeed, both in the boundary layer and the jet, squared coherence is quite small (< 0.25) over the complete frequency range when turbulence intensity is quite large whereas it is quite strong (> 0.5) over a large range of frequencies when turbulence intensity is quite small and the correlation

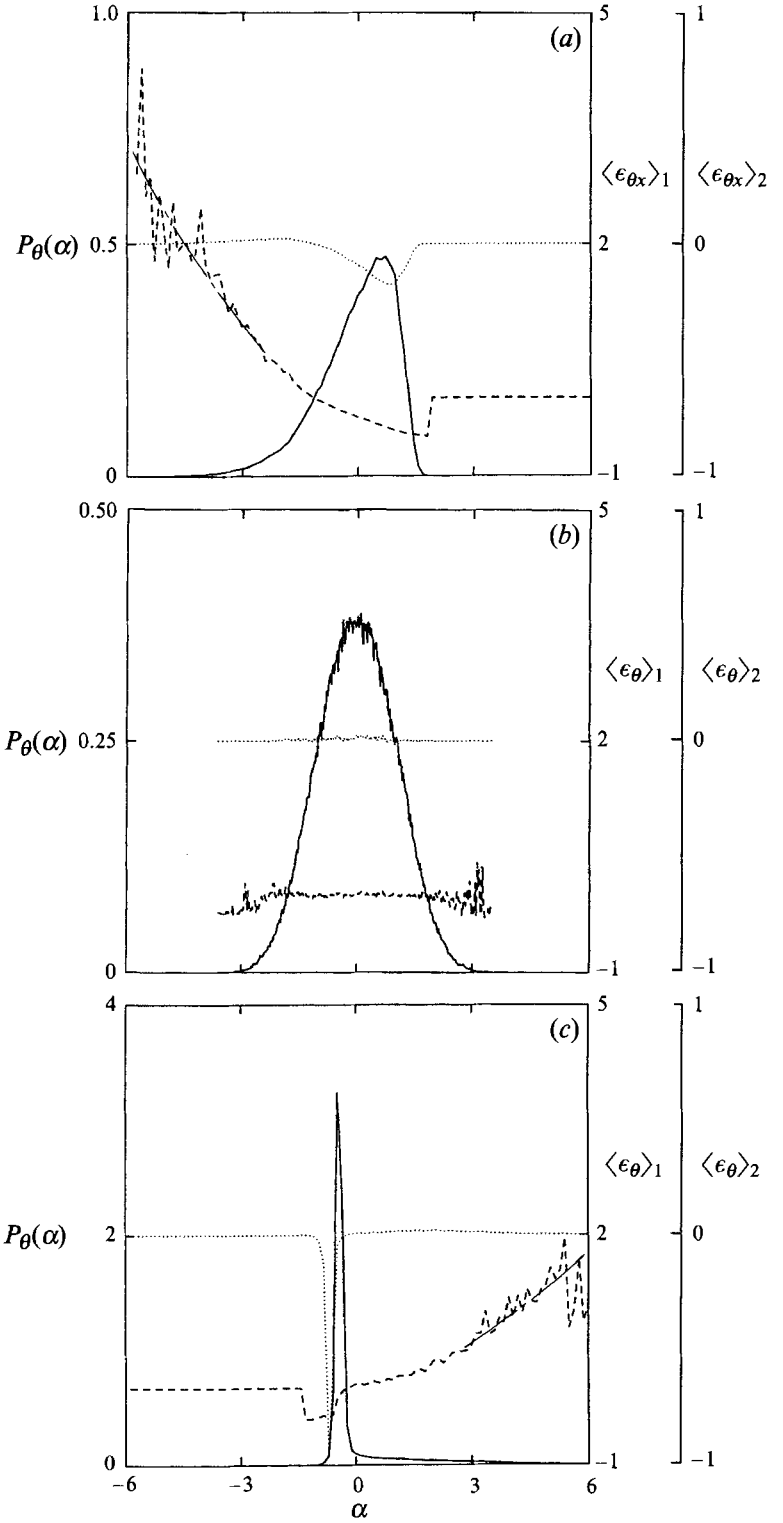

FIGURE 9. Conditional dissipations and marginal temperature p.d.f. in the boundary layer. (*a*) $y^+ = 3$; (*b*) $y^+ = 60$; (*c*) $y/\delta \approx 0.75$; ——, $\langle \epsilon_\theta \rangle_1$; ·····, $\langle \epsilon_\theta \rangle_2$; —·—, mean trend for $|\alpha| > 3$; ——, marginal temperature p.d.f.

coefficient is large in magnitude (Djeridi 1992). In addition, the imaginary parts of the cross-spectra have the negative sign in the boundary layer and the positive one in the jet, and this sign is always the same in any particular flow, regardless of the considered position. As a consequence, the phase between temperature and its dissipation varies between $-180°$ and $0°$ in the boundary layer (figure 10*a*) and between $0°$ and $+180°$ in the jet (figure 10*b*), which shows that the link between these two quantities also depends on the type of flow. Furthermore, these phase distributions are remarkably flat over a quite large range of frequencies, with oscillations for the highest frequencies for which spectral coherency becomes too small. Figure 10(*c*) presents a schematic diagram showing the relative influence of the cospectrum and quadspectra at various positions in these two flows. Though detailed results were only reported for a few typical positions in this paper, we do believe that these trends are associated with a continuous evolution between these configurations as shown on this diagram.

This result can be quite well understood if one considers that $(\partial\theta/\partial t)^2$ represents ϵ_θ. Indeed, the quadspectrum $Qu_{\theta,(\partial\theta/\partial t)^2}(f)$ between θ and $(\partial\theta/\partial t)^2$ is then equivalent (except for the multiplication by frequency f) to the cospectrum $Co_{(\partial\theta/\partial t),(\partial\theta/\partial t)^2}(f)$ between $(\partial\theta/\partial t)$ and $(\partial\theta/\partial t)^2$ since $(\partial\theta/\partial t)$ is in quadrature with respect to θ. The integral over all frequencies of this cospectrum is proportional to the skewness factor of $(\partial\theta/\partial t)$ which is known to significantly differ from zero in turbulent shear flows, though it should be zero in isotropic turbulence, owing to the asymmetric distribution of strong temporal temperature gradients associated with discontinuities commonly called 'ramps' (e.g. Mestayer *et al.* 1976; Antonia & Van Atta 1978). There is sufficient evidence showing that these ramps result from the boundary conditions so that, in a boundary layer over a heated wall and in a heated jet, they are of opposite sign. For both our boundary layer and our jet, the skewness factors $S_{\partial\theta/\partial t}$ were found to be in very good agreement ($|S_{\partial\theta/\partial t}| \approx 1$ for $R_\lambda \approx 100$–200) with the compilation of data presented by Sreenivasan (1991). Figures 10(*a*) and 10(*b*) even show that the presence of the ramps is more apparent in the regions where temperature p.d.f.s are almost Gaussian and the velocity field is almost isotropic since, at these positions, the measured quadspectra are largest as cospectra are very small: obviously, one signal such as $(\partial\theta/\partial t)^2$ cannot be strongly correlated with both another signal and this signal time derivative. At the other positions, where temperature fluctuations are much more asymmetric, this phenomenon appears to be relatively less important as the dominant feature is then the temperature asymmetry. Here again, similar behaviour is obtained for any other terms associated with dissipation ($\epsilon_{\theta y}$, $\epsilon_{\theta z}$ or ϵ_θ) as these positive quantities are also associated with small scales. Their behaviour is qualitatively similar to that of $(\partial\theta/\partial t)^2$ with respect to the θ-distribution and, consequently, to the $\partial\theta/\partial t$ asymmetries as well.

4. Conclusion

Results reported in this paper show that the assumption of statistical independence of temperature θ and any component of its dissipation or its total dissipation is sound only in regions where θ-fluctuations are almost symmetrical. This result is important for various modelling problems of turbulent flows both with and without chemical reactions where statistical independence is often assumed. Indeed, the correlation coefficient between these quantities presents evolutions qualitatively similar to those of the temperature skewness factor. In regions where the correlation is strong, the interdependence results from relatively low-frequency fluctuations – lying between the

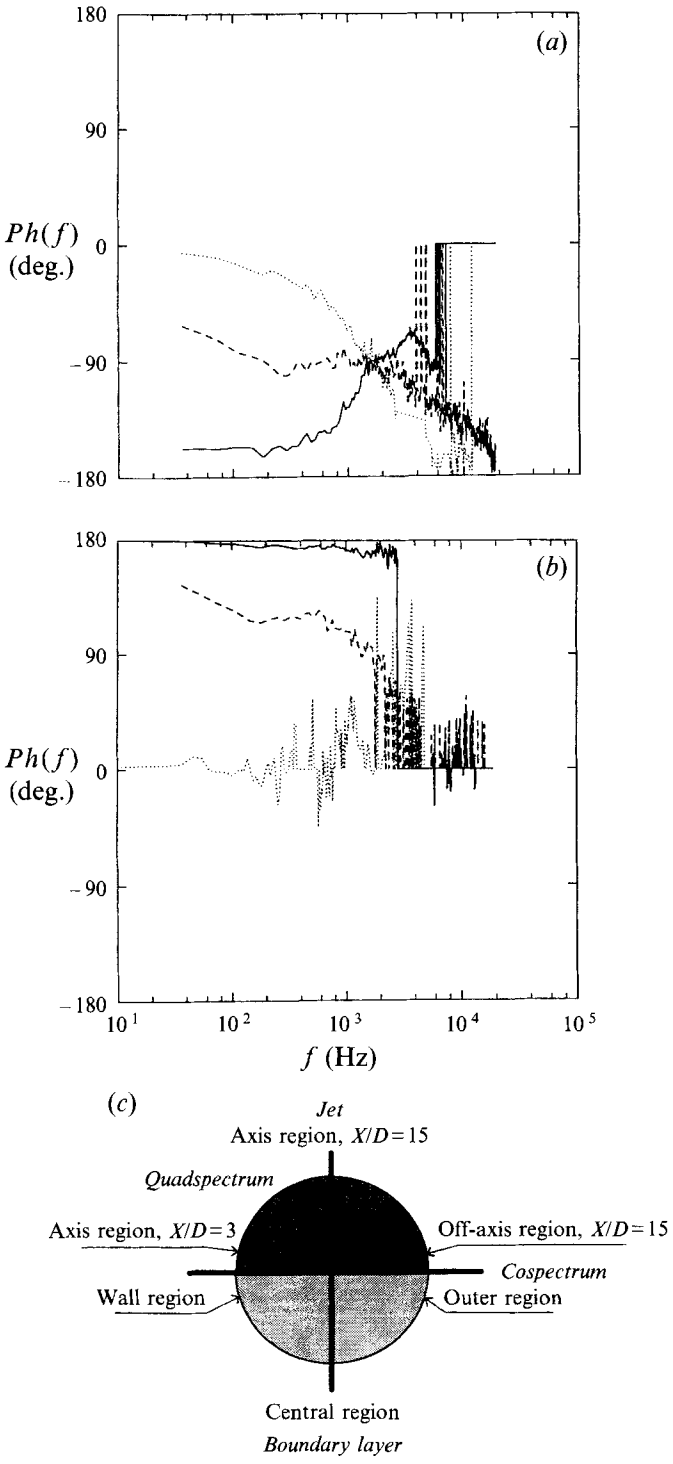

FIGURE 10. Phase between temperature and its dissipation. (*a*) Boundary layer; (*b*) jet; (*c*) schematic explanation of results. Same symbols as figure 5.

integral scale and the Taylor microscale – of small amplitude for both temperature and its squared derivatives. This seems to be associated with the low-frequency distribution of dissipation 'bursts' characteristic of small-scale intermittency since it was shown that very small dissipation fluctuations are involved. Generally speaking, similar trends were obtained in a boundary layer over a heated wall and in a heated jet. For instance, conditional dissipations show that strong fluctuations of this quantity are mainly associated with temperature fluctuations of quite large amplitude in regions where these fluctuations are asymmetrically distributed, whereas in regions where the temperature p.d.f. is almost Gaussian, though j.p.d.f. iso-contours show that large dissipation fluctuations are associated with temperature fluctuations of small amplitude, conditional dissipations are very flat as these large fluctuations are balanced by small and much more frequent ones. However, when these conditional quantities are weighted by the temperature p.d.f., they show that the main contribution to the average dissipation comes from dissipation fluctuations associated with small temperature fluctuations since those are the most frequent ones. This result is obtained both in regions where temperature fluctuations are asymmetrically distributed and in regions where they are symmetrically.

As the connection between temperature and its dissipation was found to be associated with frequencies of the order of that corresponding to Taylor's microscale, it seems that results reported in this paper will still be valid in other flows with similar boundary conditions and larger Reynolds number since the spectra for the squared derivatives will also present non-negligible low-frequency contributions in such flows. Indeed, it is well known that small-scale intermittency tends to increase with increasing Reynolds numbers (e.g. Monin & Yaglom 1975; Gagne 1987). Nevertheless, for a more fundamental approach to the problem, one of the important results is also that the link between temperature and its dissipation is related to the temperature ramps resulting from the large-scale flow boundary conditions: this effect results in phases varying between $-180°$ and $0°$ in the boundary layer and between $0°$ and $+180°$ in the jet.

Finally, we hope that results reported herein will motivate analyses in order to better determine the temporal and spatial organization of structures responsible for the observed link. Indeed, our results can be associated with other findings (e.g. George & Hussein 1991) suggesting that 'the small-scale motions remain closely related to the large-scale coherent motions, so that anisotropy could be observed over the entire spectral range if the large-scale motions are anisotropic'. It is interesting to mention that the study concerning small-scale intermittency which has been recently developed at IMST (Vaienti *et al.* 1994) may help understand these connections in more detail as it appears that the conditional-average quantity $\langle \epsilon_\theta / \Delta\theta(r) \rangle$ (where $\Delta\theta(r)$ denotes the temperature difference $\theta(x+r)-\theta(x)$, with r a separation which may lie within or outside the inertial range) is one of the terms which are important and need to be modelled when the p.d.f. transport equation for the temperature difference $\Delta\theta(r)$ is studied. Indeed, when r is large, $\Delta\theta(r)$ is equivalent to θ, whereas when r tends to η, $\Delta\theta(r)$ is equivalent to $(\partial\theta/\partial x)$.

This work is supported under grants with Electricité de France, Gaz de France and Société Nationale d'Etude et de Construction de Moteurs d'Avions. We are grateful to M. Astier for his technical assistance. The authors also gratefully acknowledge valuable discussions about this work with Professor M. Coantic.

REFERENCES

AMIELH, M., DJERIDANE, T., ANSELMET, F. & FULACHIER, L. 1994 Velocity near-field of variable density turbulent jets. *Intl J. Heat Mass Transfer* (to appear).

ANSELMET, F. & ANTONIA, R. A. 1985 Joint statistics between temperature and its dissipation in a turbulent jet. *Phys. Fluids* **28**, 1048–1054.

ANSELMET, F., DJERIDI, H. & FULACHIER, L. 1994 Simultaneous measurements of temperature and its dissipation using pairs of parallel cold wires. *Exps. Fluids* (submitted).

ANTONIA, R. A., BROWNE, L. W. B., BRITZ, D. & CHAMBERS, A. J. 1984 A comparison of temporal and spatial temperature increments in a turbulent plane jet. *Phys. Fluids* **27**, 87–93.

ANTONIA, R. A., FULACHIER, L., KRISHNAMOORTHY, L. V., BENABID, T. & ANSELMET, F. 1988 Influence of wall suction on the organized motion in a turbulent boundary layer. *J. Fluid Mech.* **190**, 217–240.

ANTONIA, R. A. & MI, J. 1993 Temperature dissipation in a turbulent round jet. *J. Fluid Mech.* **250**, 531–551.

ANTONIA, R. A., PRABHU, A. & STEPHENSON, S. E. 1975 Conditionally sampled measurements in a heated turbulent jet. *J. Fluid Mech.* **72**, 455–480.

ANTONIA, R. A. & VAN ATTA, C. W. 1978 Structure functions of temperature fluctuations in turbulent shear flows. *J. Fluid Mech.* **84**, 561–580.

BILGER, R. W. 1976 Turbulent jet diffusion flames. *Prog. Energy Combust. Sci.* **1**, 87–109.

BILGER, R. W. 1980 Turbulent flows with non premixed reactants. In *Topics in Applied Physics*, vol. 44 (ed. P. A. Libby & F. A. williams), pp. 65–113. Springer.

BILGER, R. W. 1989 Turbulent diffusion flames. *Ann. Rev. Fluid Mech.* **21**, 101–135.

BILGER, R. W. 1993 Conditional moment closure for turbulent reacting flow. *Phys. Fluids* A **5**, 436–444.

BORGHI, R. & GONZALEZ, M. 1986 Application of Lagrangian models to turbulent combustion. *Combust. Flame* **63**, 239–250.

BRAY, K. M. C. 1980 Turbulent flows with premixed reactants. In *Topics in Applied Physics*, vol. 44. (ed. P. A. Libby & F. A. Williams), pp. 115–183. Springer.

CHEN, H., CHEN, S. & KRAICHNAN, R. H. 1989 Probability distribution of a stochastically advected scalar field. *Phys. Rev. Lett.* **63**, 2657–2660.

DJERIDI, H. 1992 Etude de la liaison entre un scalaire passif et sa dissipation en écoulements turbulents libre et de paroi. PhD thesis, Université d'Aix-Marseille II.

ESWARAN, V. & POPE, S. B. 1988 Direct numerical simulations of the turbulent mixing of a passive scalar. *Phys. Fluids* **31**, 506–520.

FULACHIER, L. 1972 Contribution à l'étude des analogies des champs dynamique et scalaire dans une couche limite turbulente. Effet de l'aspiration. Thèse de Doctorat ès Sciences Physiques, Université de Provence, Marseille.

FULACHIER, L. 1978 Hot-wire measurements in low-speed heated flows. In *Proc. Dynamic Flow Conf., Marseille*, pp. 465–488. PO Box 121, DK-2740, Skovlunde, Denmark.

GAGNE, Y. 1987 Etude expérimentale de l'intermittence interne et des singularités dans le plan complexe en turbulence développée, Thèse de Doctorat ès Science, INP, Grenoble.

GAO, F. 1991 Mapping closure and non-gaussianity of the scalar probability density functions in isotropic turbulence. *Phys. Fluids* A **3**, 2438–2444.

GEORGE, W. K. & HUSSEIN, H. J. 1991 Locally axisymmetric turbulence. *J. Fluid Mech.* **233**, 1–23.

HANNART, B., GAGNE, Y. & HOPFINGER, E. J. 1985 Domaine d'existence de l'isotropie dans une couche de mélange turbulente. *C.R. Acad. Sci. Paris* II, **301**, 669–674.

JACQUIN, L. 1983 Etude du comportement intermittent de la dissipation dans une couche limite à grand nombre de Reynolds, PhD thesis, Université d'Aix-Marseille II.

JAYESH & WARHAFT, Z. 1992 Probability distribution, conditional dissipation, and transport of passive temperature fluctuations in grid-generated turbulence. *Phys. Fluids* A **4**, 2292–2307.

KLEWICKI, J. C. & FALCO, R. E. 1990 On accurately measuring statistics associated with small-scale structure in turbulent boundary layers using hot-wire probes. *J. Fluid Mech.* **219**, 119–142.

KRISHNAMOORTHY, L. V. & ANTONIA, R. A. 1987 Temperature dissipation measurements in a turbulent boundary layer. *J. Fluid Mech.* **176**, 265–281.

KUZTNETSOV, V. R., PRASKOVSKY, A. A. & SABELNIKOV, V. A. 1992 Fine-scale turbulence structure of intermittent shear flows. *J. Fluid Mech.* **243**, 595–622.

MESTAYER, P. & CHAMBAUD, P. 1979 Some limitations to measurements of turbulence microstructure with hot and cold wires. *Boundary-Layer Met.* **16**, 311–329.

MESTAYER, P., GIBSON, C. H., COANTIC, M. & PATEL, A. S. 1976 Local anisotropy in heated and cooled turbulent boundary layers. *Phys. Fluids* **19**, 1279–1287.

MONIN, A. S. & YAGLOM, A. M. 1975 *Statistical Fluid Mechanics: Mechanics of Turbulence*, vol. 2. MIT Press.

NAMAZIAN, M., SCHEFFER, R. W. & KELLY, J. 1988 Scalar dissipation measurements in the developing region of a jet. *Combust. Flame* **74**, 147–160.

O'BRIEN, E. E. & SAHAY, A. 1992 Asymptotic behaviour of the amplitude mapping closure. *Phys. Fluids* A **4**, 1773–1775.

PANCHAPAKESAN, A. & LUMLEY, J. L. 1993 Turbulence measurements in axisymmetric jets of air and helium. *J. Fluid Mech.* **246**, 225–247.

PIOMELLI, U., BALINT, J. L. & WALLACE, J. M. 1989 On the validity of Taylor's hypothesis for wall-bounded flows. *Phys. Fluids* A **1**, 609–611.

POPE, S. B. & CHEN, Y. L. 1990 The velocity-dissipation probability density function model for turbulent flows. *Phys. Fluids* A **2**, 1437–1449.

RUFFIN, E., SCHIESTEL, R., ANSELMET, F., AMIELH, M. & FULACHIER, L. 1994 Investigation of characteristic scales in variable density turbulent jets using a second-order model. *Phys. Fluids* **6**, 2785–2799.

SAHAY, A. & O'BRIEN, E. E. 1993 Uniform mean scalar gradient in grid turbulence: conditioned dissipation and production. *Phys. Fluids* A **5**, 1076–1078.

SREENIVASAN, K. R. 1991 On local isotropy of passive scalars in turbulent shear flows. *Proc. R. Soc. Lond.* A **434**, 165–182.

SREENIVASAN, K. R., ANTONIA, R. A. & DANH, H. Q. 1977 Temperature dissipation fluctuations in a turbulent boundary layer. *Phys. Fluids* **20**, 1238–1249.

VAIENTI, S., OULD-ROUIS, M., ANSELMET, F. & LE GAL, P. 1994 Statistics of temperature increments in fully developed turbulence. Part I. Theory. *Physica D* **73**, 99–112.

VEROLLET, E. 1972 Etude d'une couche limite turbulente avec aspiration et chauffage à la paroi. Thèse de Docteur ès Sciences Physiques, Université de Provence, Marseille.

VRANOS, A. 1992 A generalised conditional scalar dissipation-mixture fraction joint pdf for flamelet modelling of non-premixed flames. *Combust. Sci. Tech.* **84**, 323–334.

WARHAFT, Z. & LUMLEY, J. L. 1978 An experimental study of the decay of temperature fluctuations in grid-generated turbulence. *J. Fluid Mech.* **88**, 659–684.

WYNGAARD, J. C. 1971 Spatial resolution of a resistance wire temperature sensor. *Phys. Fluids* **14**, 2052–2054.